

## ORIGINAL ARTICLE

# Mutational profiling of bone metastases from lung adenocarcinoma: results of a prospective study (POUMOS-TEC)

Cyrille B Confavreux<sup>1,2</sup>, Nicolas Girard<sup>3</sup>, Jean-Baptiste Pialat<sup>1,4</sup>, Pierre-Paul Bringuier<sup>5,6</sup>, Mojgan Devouassoux-Shisheboran<sup>6,7</sup>, Jean-Charles Rousseau<sup>1</sup>, Sylvie Isaac<sup>8</sup>, Françoise Thivolet-Bejui<sup>9</sup>, Philippe Clezardin<sup>1</sup> and Marie Brevet<sup>1,9</sup>

<sup>1</sup>Inserm UMR1033-Université de Lyon, Lyon, France. <sup>2</sup>Rheumatology Department, Hôpital Edouard Herriot, Hospices Civils de Lyon, Lyon, France. <sup>3</sup>Respiratory Medicine, Thoracic Oncology Department, Hôpital Louis Pradel, Hospices Civils de Lyon, Lyon, France. <sup>4</sup>Radiology Department, Hôpital Edouard Herriot, Hospices Civils de Lyon, Lyon, France. <sup>5</sup>Pathology Department, Molecular Diagnostics Platform, Hôpital Edouard Herriot, Hospices Civils de Lyon, Lyon, France. <sup>6</sup>Cancer Research Center of Lyon (CRCL), Lyon, France. <sup>7</sup>Pathology Department, Hôpital de la Croix Rousse, Hospices Civils de Lyon, Lyon, France. <sup>8</sup>Pathology Department, Centre Hospitalier Lyon Sud, Hospices Civils de Lyon, Lyon, France. <sup>9</sup>Pathology Department, Groupement Hospitalier Est, Hospices Civils de Lyon, Lyon, France.

Targeted therapies have improved patient survival in metastatic lung adenocarcinoma. Molecular diagnosis is a key element to identify oncogenic drivers predicting the efficacy of these agents. In stage IV patients, histopathological diagnosis is often performed on bone metastases biopsy, but routine procedure of decalcification may alter DNA quality for subsequent molecular tests. We set up a procedure to perform molecular analyses on bone metastasis and describe the results of mutational profiling. POUMOS-TEC is a prospective study conducted in stage IV lung adenocarcinomas. Bone metastasis specimens from surgery and CT-scan guided biopsies were sent fresh for immediate formalin-fixation. Decalcification was performed, only when necessary, using EDTA. Controls were processed with acid decalcification. DNA extraction was performed after laser microdissection. Mutational profiling of oncogenic drivers was conducted as recommended by the French National Cancer Institute. Diagnosis efficiency of the computed tomography (CT)-scan guided biopsy process was assessed. Among 177 collected bone metastases specimens, 49 came from lung adenocarcinomas. Specimens processed with no decalcification or EDTA ( $n = 45$ ) provided high-quality DNA. Molecular profiling was performed in 44/45 (98%) of cases. The results of the whole panel of oncogenic drivers (*EGFR*, *KRAS*, *BRAF*, *PIK3CA*, *HER2* and *ALK*) were obtained in 41/45 (91%) of cases. A mutation was observed in 50% of cases including 32% of *KRAS* and 14% of epidermal growth factor receptor (*EGFR*) mutations. CT-scan biopsy efficiency rate was 96%. We demonstrated the feasibility to routinely conduct mutational profiling on bone metastases biopsies. We observed a higher rate of *EGFR* mutations (+ 42%) in comparison with the average rate of all stage IV lung adenocarcinomas. This procedure is a new step toward the goal of personalized medicine to treat lung cancers and other osteophilic tumors.

BoneKEy Reports 3, Article number: 580 (2014) | doi:10.1038/bonekey.2014.75

## Introduction

Molecular profiling of oncogenic drivers, including mutations occurring in the epidermal growth factor receptor (*EGFR*) gene and rearrangements of the anaplastic lymphoma kinase (*ALK*) gene, is systematically recommended in the pretherapeutic workup of metastatic lung adenocarcinoma [http://www.nccn.org/professionals/physician\\_gls/pdf/nscl.pdf](http://www.nccn.org/professionals/physician_gls/pdf/nscl.pdf),<sup>1</sup> as patients may then benefit from specific agents targeting these alterations that provide with high response rates and prolonged survival.<sup>2</sup> With the emerging field of personalized medicine in oncology and the increasing number of described mutations, large-scale

org/professionals/physician\_gls/pdf/nscl.pdf,<sup>1</sup> as patients may then benefit from specific agents targeting these alterations that provide with high response rates and prolonged survival.<sup>2</sup> With the emerging field of personalized medicine in oncology and the increasing number of described mutations, large-scale

Correspondence: Dr CB Confavreux, Department of Rheumatology, INSERM UMR1033—Université de Lyon, Pavillon F, Hôpital Edouard Herriot, 5 place d'Arsonval, Lyon 69003, France.  
E-mail: [cyril.confavreux@inserm.fr](mailto:cyril.confavreux@inserm.fr)

Received 20 May 2014; accepted 27 July 2014; published online 1 October 2014

mutational profiling methods arise. Thus, getting high-quality tumor DNA at the primary or the metastatic site is crucial to guide treatment decision making.<sup>3</sup>

Bone metastases are reported to occur in 30–50% of lung adenocarcinomas and may be synchronous in up to 15% of cases.<sup>4–6</sup> Patients may require metastasis biopsy, when the primary pulmonary tumor is not accessible or when access to the primary lung tumor is precluded by co-morbidities. Pathological and molecular diagnoses are then performed on specimens from metastatic lesions, but the feasibility of performing accurate molecular diagnoses on small-biopsy specimens from bone metastases has been questioned over time.<sup>6</sup> Indeed, acid-based proprietary agent (RDO) is used in most pathology departments worldwide in order to soften the bone tissue. The main disadvantage of these RDO decalcifiers is the alteration of DNA structure, which prevents any subsequent molecular analyses.<sup>7,8</sup>

Here, we set up a prospective cohort—further referred as POU MOS-TEC—to evaluate the feasibility of mutational profiling assessment on bone metastases of lung adenocarcinoma in a routine practice, using an alternative decalcification method when necessary and provide the first oncogenic driver profile of bone metastases from lung adenocarcinoma.

## Results

### Population characteristics

Among the 177 specimens of bone metastases that were collected under the POU MOS-TEC study, there were 49 bone metastases of lung adenocarcinoma. Twelve (24%) specimens were obtained from surgery, usually in the setting of treatment or prevention of acute skeletal event, and 37 (76%) from computed tomography (CT)-guided bone biopsy. Twenty-one (43%) specimens were decalcified using the EDTA experimental procedure and 24 (49%) did not require decalcification. As control, two specimens in each group were decalcified using RDO decalcification by nitric acid. In addition, frozen samples were realized in 31 cases (27 biopsies and four surgery specimens) (Figure 1).

### Histopathology analysis

All included tumors were of adenocarcinoma subtype assessed by morphology and immunohistochemical expression. Tumor

cells were organized in small sheets next to the bone trabeculae, in glands, or had massively infiltrated bone tissue (Figure 2b). In case 45, we only observed lymphatic tumor embols (Figure 2a). Cytokeratin 7 was positive for all cases (Figure 2c). TTF1 expression status was obtained for 47 cases (96%), with a TTF1 expression in 30 cases (61%) (Figure 2d). For TTF1-negative cases, the pulmonary origin of the metastasis was confirmed by histology on primary tumor and/or high radiological and clinical suspicion.

### Molecular diagnosis efficiency

In the four control specimens decalcified using RDO (nitric acid), 100% did not provide with sufficient high-quality DNA to perform molecular analysis. Poor quality DNA was assessed either by the impossibility to obtain PCR amplification visualized on gel or by the impossibility to analyze the sequencing data because of important background. By contrast, using our process of EDTA decalcification or no decalcification, DNA quality was high and sequences could be easily analyzed. A complete molecular profiling, including *EGFR*, *KRAS*, *BRAF*, *PIK3CA* and *HER2* mutations and *ALK* rearrangements, was feasible in 91% (41/45) of cases. In three patients—two in EDTA and one not decalcified—the whole set of molecular analyses could not be performed (only *EGFR* was performed for these three patients) because of an insufficient amount of tumors and only one sample in EDTA did not provide sufficient material to perform molecular analysis. Thus, a molecular profiling was obtained in 98% (44/45) of cases (Table 1).

### Mutational profiling of bone metastases of lung adenocarcinoma

Molecular characteristics of the 49 bone samples are detailed in Table 1. Among the 44 evaluable cases, 22 (50%) harbored at least one molecular alteration of the panel. *KRAS* mutations were the most frequent (32% of cases) (Figure 3f). *EGFR* mutations were observed in 14% of cases (Figure 3a) and *HER2* and *BRAF* mutations in one (2%) case each. *ALK* rearrangement by fluorescent *in situ* hybridization was observed in one (2%) case, also exhibiting *ALK* expression at immunohistochemistry (Figures 3k and l). No *PIK3CA* mutation was observed. Comparison of mutational profiling between

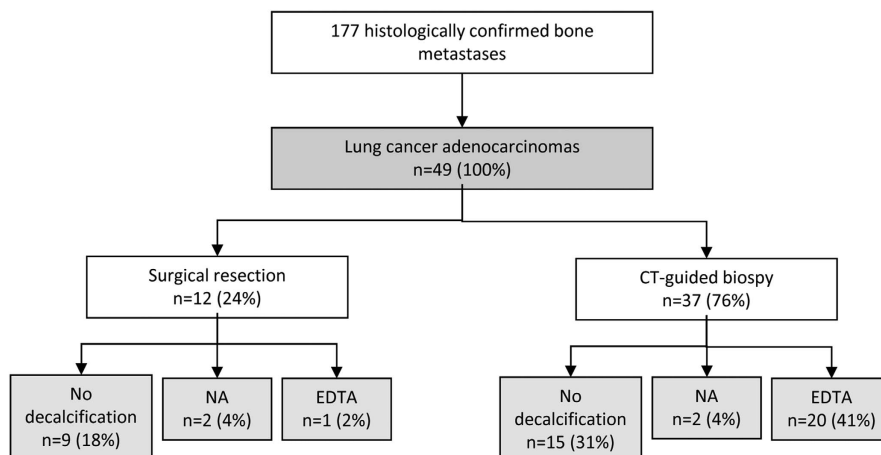
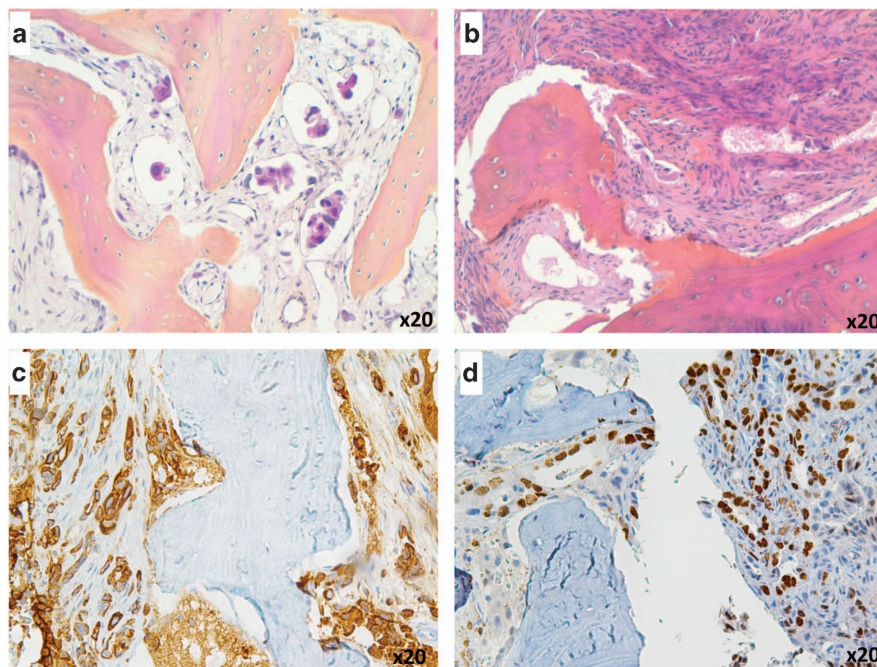


Figure 1 Description of the population of POU MOS-TEC study.



**Figure 2** Histopathologic features of bone metastases (a, b) in cases 45 and 41 (H&E). (c, d) Cytokeratin 7 and TTF1 immunohistochemistry on case 35, showing cytoplasmic and nuclear expression, respectively, in 100% of tumoral cells.

EDTA-decalcified and no decalcified samples has been summarized in **Table 2**.

#### Diagnosis efficiency of CT-scan guided bone biopsies

Among the 93 biopsies, 46 patients were referred with a suspected lung cancer on the basis of chest-CT-scan with a highly suspect pulmonary tumor mass (**Figure 4**). The procedure provided between one and four fresh bone samples for each patient with a mean of two biopsies per patient. Four patients (8.7%) corresponded to another diagnosis. Forty cases (87%) were histologically confirmed as metastatic lung cancers including 37 (80%) adenocarcinomas, two squamous and one small cell carcinoma. There were only two biopsy failures (4.3%) because of the absence of material or normal tissue. Thus, the efficiency rate of our CT-scan guided bone biopsy network was 96% (44/46) (**Figure 4**). Procedure was safe as no grade 3–4 adverse event occurred.

#### Discussion

This study is, to our knowledge, the first cohort of bone metastases from lung adenocarcinoma characterized for major oncogenic driver molecular alterations. Our results, besides demonstrating the feasibility of using bone metastasis specimens to perform histopathological and molecular diagnosis of lung adenocarcinoma in a routine practice setting, indicate that 50% of cases harbored at least one oncogenic mutation, including 14% of *EGFR* mutations. Overall, CT-scan guided bone biopsy had a diagnostic efficiency rate of 96%.

Up to now, the decalcification routine technique was not such a problem, as it had no impact on morphological and immunohistochemical results.<sup>9,10</sup> The emergence of personalized medicine using targeted agents highlighted the relevance to preserve DNA quality even after extraction from bone biopsy.

Thus, decalcification process became a critical point. As expected, RDO-decalcifiers severely altered DNA quality. We chose EDTA decalcification because it provides with good morphological results and high-quality DNA to perform molecular analysis.<sup>7,8,11</sup> We obtained morphology, immunohistochemistry, molecular analysis and fluorescent *in situ* hybridization of high quality on EDTA-decalcified samples. In our series, the absence or the partial molecular analysis was not due to poor quality of DNA but only to limited quantity of tissue. Surprisingly, EDTA is not commonly used in pathology laboratories, probably because EDTA decalcification is taking much more time compared with decalcification by RDO-decalcifiers.<sup>10</sup> Nevertheless, in our experience, using EDTA-decalcification method, a CT-guided bone biopsy could be processed within 2 days.

Our study provides an original insight on oncogenic driver profiles in patients with synchronous bone metastases from lung adenocarcinoma. Interestingly, a druggable target was observed in 50% of cases, which is roughly what is observed in the primary tumor in France.<sup>12</sup> That is of particular clinical relevance as patients presenting with synchronous bone metastases usually present with initial poor performance status, sometimes contra-indicating cytotoxic chemotherapy to be safely delivered; this may not be the case for targeted therapy in the setting of *EGFR*- or *ALK*-driven tumors. It is noteworthy that *EGFR* mutations were more frequent (+42%) in comparison with the global incidence of these mutations in metastatic lung adenocarcinoma in France.<sup>12</sup> Some smaller studies reported similar rates in the metastatic setting, but molecular characterization was not performed on bone metastasis samples.<sup>13,14</sup> These data need to be confirmed in larger cohorts of patients. One limitation of the study was the absence of comparison between RDO and EDTA decalcification for the same biopsy. This was due to the routine practice setting of our



**Table 1** Results of molecular profiling

Patient	Sample	Decalcification	Mutation profile
1	SR	—	KRAS G12D
2	SR	—	—
3	CT	—	EGFR E746_A750del
4	CT	—	—
5	SR	—	KRAS G12A
6	CT	—	—
7	SR	—	KRAS G12A
8	SR	—	—
9	SR	—	—
10	CT	—	—
11	CT	—	NCP
12	CT	—	KRAS G12C
13	CT	—	KRAS G13D & BRAF D594G
14	CT	—	KRAS G12C
15	CT	—	—
16	CT	—	KRAS G12C
17	CT	—	—
18	CT	—	KRAS G12V
19	CT	—	EGFR E746_A750del
20	CT	—	KRAS G12V
21	SR	—	—
22	SR	—	EGFR L858R & T790M
23	CT	—	KRAS G12V
24	CT	—	—
25	CT	EDTA	EGFR E746_A750del
26	CT	EDTA	KRAS G12V
27	CT	EDTA	EGFR L747_P753del
28	CT	EDTA	KRAS G13D
29	CT	EDTA	NCP
30	CT	EDTA	—
31	CT	EDTA	—
32	CT	EDTA	NCP
33	CT	EDTA	—
34	CT	EDTA	—
35	CT	EDTA	—
36	CT	EDTA	KRAS G13D
37	CT	EDTA	EML4-ALK
38	CT	EDTA	—
39	CT	EDTA	EGFR L858R
40	CT	EDTA	KRAS G12C
41	CT	EDTA	—
42	SR	EDTA	—
43	CT	EDTA	—
44	CT	EDTA	NP
45	CT	EDTA	HER2 A775_G776insYVMA
46	SR	RDO	NI
47	SR	RDO	NI
48	CT	RDO	NI
49	CT	RDO	NI

Abbreviations: CT, CT-guided biopsy; NCP, not completely performed; NI, not interpretable; NP, not performed; SR, surgery resection.

study and the ethical necessity to optimize the chance to get the diagnosis for the patient, as quantity of tumor cells is a critical point for the molecular diagnosis efficiency.

CT-guided bone metastasis biopsy represents a safe and a valuable option to make a histopathological and molecular diagnosis in patients presenting lung tumors with synchronous bone metastasis. Indeed, these patients frequently suffer from emphysema, respiratory failure or other co-morbidities precluding standard diagnostic procedures, such as fiberoptic bronchoscopy or percutaneous biopsy of the lung tumor, to be safely conducted.<sup>5</sup> In addition, whenever an interventional procedure, such as cementoplasty, is required for pain management, bone biopsy would then be part of the radiological procedure. To obtain sufficient and adequate material, we targeted the border of the lesions, where tumor burden is the

most active, as we noticed that the center of bone metastasis is easily made of altered necrotic tissues of poor quality for histological analysis; tumor burden on Pet-scan images was commonly larger compared with the osteolytic area on CT-scan images. Several passages may be recommended to obtain sufficient amount of material.

The increased rate of *EGFR* mutation raises the issue that lung adenocarcinomas may have different metastatic patterns according to mutational profiling. In a recent series of molecularly defined lung adenocarcinomas reporting on clinical-genotype correlations, *ALK* rearrangements have been associated with more frequent liver and pleural metastases, whereas *EGFR* mutation tended to be more frequent in case of bone metastases ( $P=0.08$ ).<sup>15</sup> This is in line with our observations suggesting that *EGFR*-mutated adenocarcinoma cells may have an increased bone affinity. In addition, some observations of patients responding to *EGFR* inhibitor presenting with condensation of their bone metastases<sup>16</sup> suggest that there may be specific interactions between *EGFR*-mutated cells and the bone microenvironment. In another study, the absence of treatment with *EGFR* tyrosine kinase inhibitor was associated with more skeletal-related events and a reduced time to first skeletal-related event (3.3 vs 11.8 months,  $P<0.001$ ).<sup>17</sup> Relationships between bone microenvironment and *EGFR*-mutant adenocarcinoma cells remain poorly understood. A hypothesis is that the release of EGF-like factors alters the osteoprotegerin—RANKL ratio.<sup>18</sup> There is a need to set up new animal models of lung metastatic bone cancers to decipher this interaction.<sup>4,19</sup>

To conclude, using EDTA-decalcification method, we provide for the first time data on oncogenic drivers in patients with synchronous bone metastases from lung adenocarcinoma. Our results highlight the higher rate of *EGFR* mutation in these patients. Our technique for the processing of bone biopsies is reliable on both CT-guided bone biopsies and surgery pieces and provides with a major tool toward the goal of personalized medicine to treat lung cancers and other osteophilic tumors requiring molecular profiling.

## Subjects and Methods

### POUMOS-TEC

POUMOS-TEC is a prospective multidisciplinary cohort conducted at the Hospices Civils de Lyon-France between 1 April 2011 and 1 May 2013. The aim of the study was to set up a global diagnostic approach regarding bone metastases from lung adenocarcinomas to obtain systematic molecular profiling of major oncogenic drivers. The study was approved by the local ethic committee of Lyon. Specimens were primarily obtained from surgical resection or CT-guided bone biopsy. Patients undergoing a bone metastasis biopsy (by CT or surgery) in the setting of routine diagnosis were all screened, but POUMOS-TEC only included patients with histologically proven lung adenocarcinoma.

### CT-guided bone biopsy process

Target site for bone biopsy was evaluated beforehand on CT images, and target selection was based on its accessibility and its cellular pattern (contrary to a necrotic pattern). Using a 14-gauge bone biopsy needle, the ideal biopsy path carried the boundary between healthy and pathological bone area. In

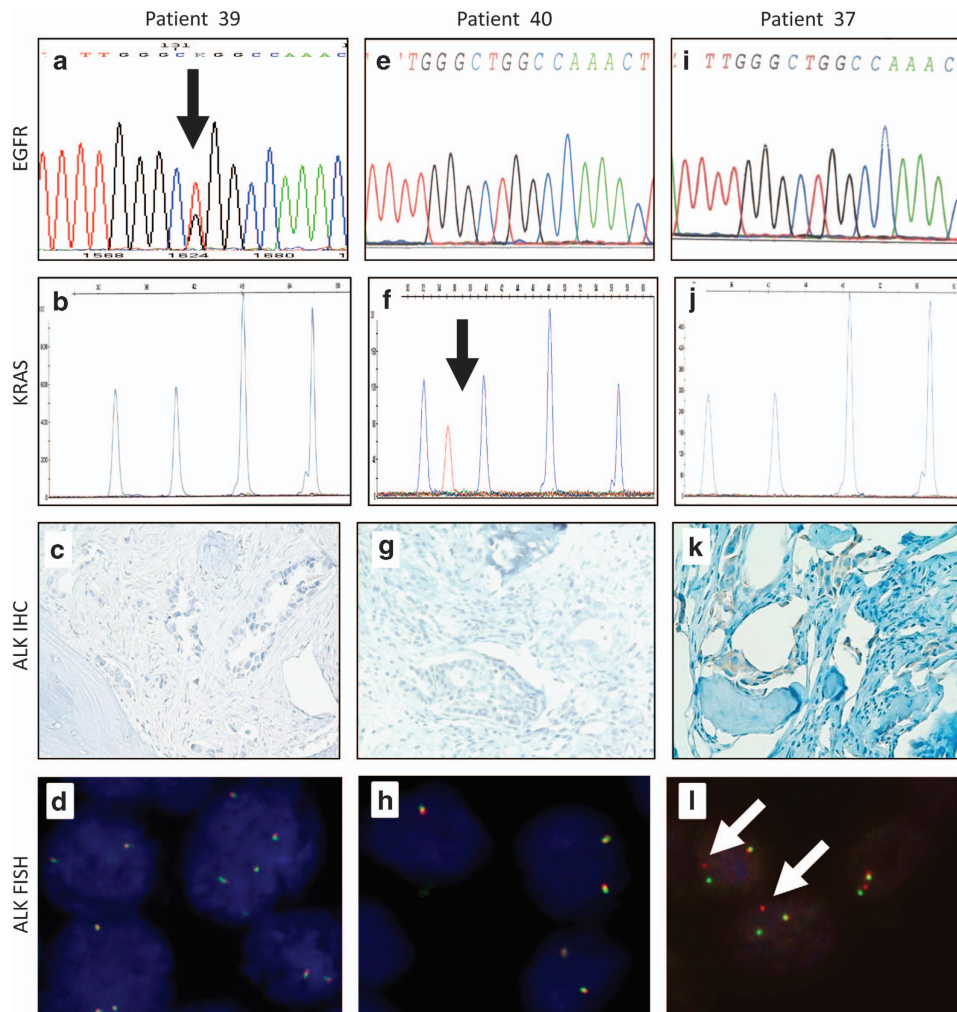


**Figure 3** Example of bone metastasis molecular analysis profiling of three different patients. Analysis of patient 39 showed (a) a L858R mutation (arrow) in sens exon 21 EGFR sequence but (b) normal KRAS SNaPshot analysis and (c, d) the absence of EML4-ALK translocation. Analysis of patient 40 showed (f) a KRAS G12C mutation (arrow) by SNaPshot analysis, (e) a normal exon 21 EGFR sequence and (g, h) the absence of EML4-ALK translocation. Analysis of patient 37 showed an EML4-ALK translocation by (i) FISH analysis (X100) (arrow) and (k) immunohistochemistry with a 100% expression on tumor cells (X40). In this patient, (l) exon 21 EGFR sequence and (j) KRAS SNaPshot analysis were normal.

**Table 2** Comparison of mutation rates obtained in EDTA-decalcified samples and no decalcified samples

	EGFR	KRAS	BRAF	HER2	PIK3CA	ALK	Total
No decalcification (n = 24)	3 (12,5)	10 (41,6)	1 (4,1)	0 (0)	0 (0)	0 (0)	13 (54,1)
EDTA (n = 20)	3 (15)	4 (20)	0 (0)	1 (5)	0 (0)	1 (5)	9 (45)
Total (n = 44)	6 (13,6)	14 (31,8)	1 (2,3)	1 (2,3)	0 (0)	1 (2,3)	22 (50)

addition, when the patient had significant localized pain, the biopsy focused on the painful site with consecutive treatment by percutaneous cementoplasty (**Figure 5**). For more details please see Supplementary Methods.

### Pathology procedure

For all suspected bone metastases of lung cancer, surgeons and radiologists were asked to send fresh specimens in humidified sterile compresses to the pathology department. Maximum transfer time allowed was 1 h. The pathologist

checked specimen for snap-freezing in the Tissue Bank (Biological Ressource Center) and processed formalin-fixation (10% pH 7.2) for a minimum of 6 h for biopsies and 48 h for surgical pieces. Next, decalcification of bone was performed using EDTA (0.5M EDTA pH8.0, Promega, Madison, WI, USA) during a minimum of 4 h for CT biopsies to 4 days for the surgical piece. EDTA was chosen for a better preservation of cell morphology and DNA. No decalcification was performed when the bone biopsy seems soft at the macroscopic examination corresponding most of the time at a major osteolysis or

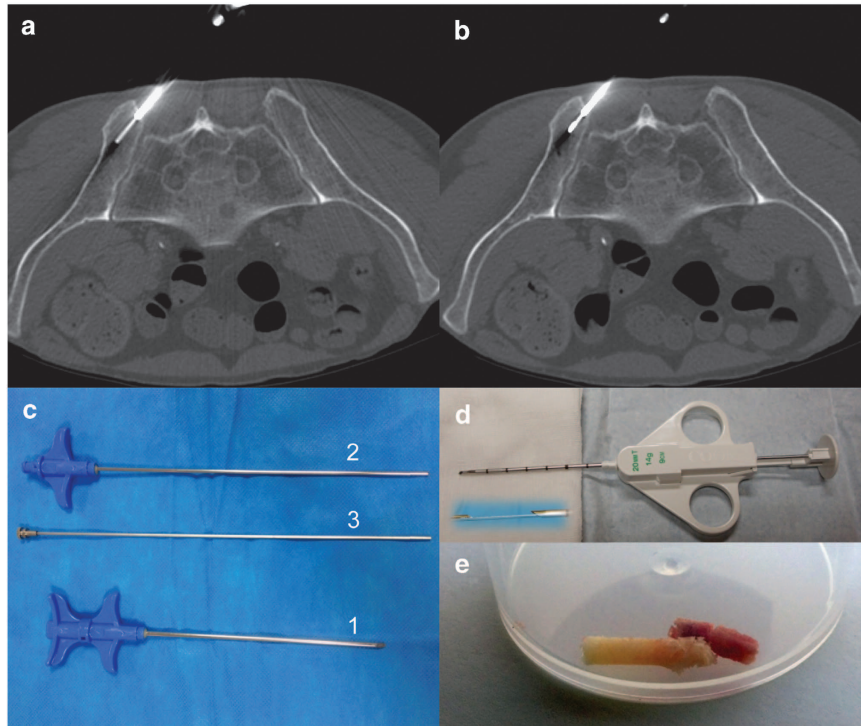


**Figure 4** Technique of bone biopsy guided by CT-scan. (a, b) The trocar is set up adjacent to the lesion, and the biopsy needle is used to drill the lesion and to get a bone sample. When no correct bone sample is obtained (tissular lytic lesion), a semi-automatic biopsy-gun is introduced within the trocar to get tumoral tissue samples. (c) 14-gauge bone biopsy needle set with the trocar (1), the biopsy needle (2) and the pusher (3) to extract the bone sample. (d) 14-gauge semi-automatic biopsy-gun used for massive lytic soft tissue-like lesions. (e) Bone specimens obtained from CT-guided bone biopsy.

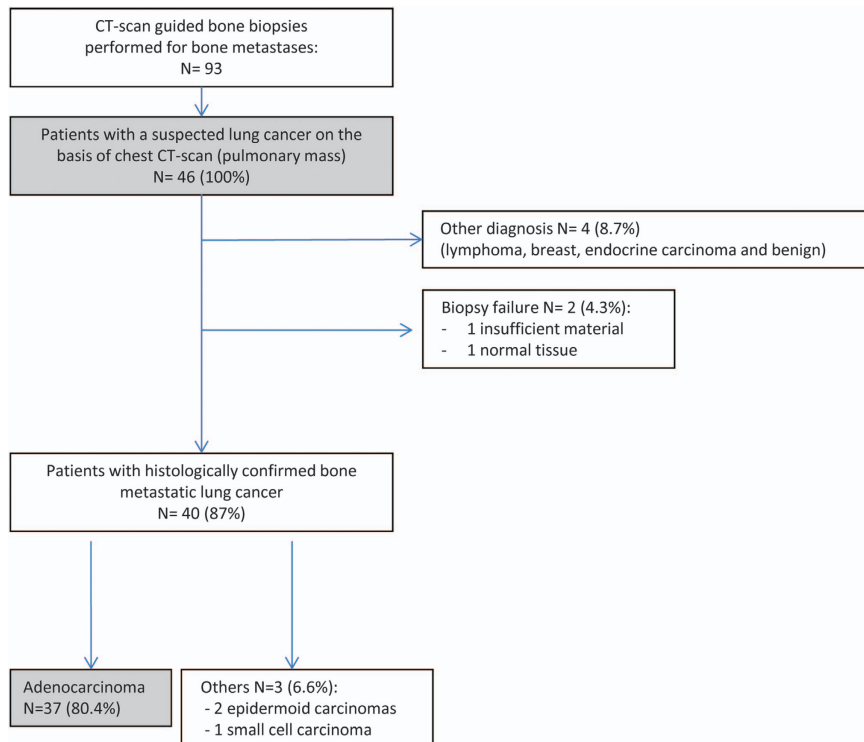


**Figure 5** Diagnosis efficiency of CT-scan guided bone biopsies to confirm histology of bone metastases from non-small cell lung cancers (NSCLCs) between 1 April 2011 and 1 May 2013.



massively tumoral infiltration. The decision to decalcify relied on gross assessment and the ability to transpierce the sample using 25-gauge needle. Decalcification was performed whenever the needle could not pierce the sample. In parallel, two specimens from surgery resection and two specimens from CT-guided bone biopsy were processed through the conventional procedure using RDO decalcification (24–48 h duration). Then, all specimens were dehydrated and paraffin embedded according to routine procedure. For EDTA-decalcified specimens, no acid solution was used at any steps of the protocol.

### Staining and immunohistochemistry

For routine histological and immunohistochemical diagnoses, 3- $\mu\text{m}$  block sections were stained with Hematoxylin, Eosin, Safran. Immunohistochemical analysis for TTF1, cytokeratin 7 and ALK was performed. Briefly, 3- $\mu\text{m}$ -thick sections of formalin-fixed and paraffin-embedded tissue samples were realized. The immunohistochemical staining was performed on a Ventana XT immunostainer, using antibodies against TTF1 (clone 8G7G3/1, Thermo Fisher Scientific, Waltham, MA, USA; 1/75), Cytokeratin 7 (clone OV-TL12/30, DAKO, Glostrup, Denmark; 1/400) and ALK (clone 5A4, Abcam, Cambridge, UK; 1/50). Then, the avidin-biotin-peroxydase complex technique was used. Reactions were developed using a chromogenic reaction in DAB (diamino-3,3'-benzidine tetrachlorhydrate) substrate solution (DAB, Sigma Fast). The counterstain was performed with hematoxylin solution.

### Molecular techniques

Mutational profiling for *EGFR*, *HER2*, *PIK3CA*, *BRAF* and *KRAS* mutations, as well as fluorescent *in situ* hybridization analysis for *ALK* gene rearrangements, is recommended in France as part of routine good clinical practice for the diagnosis of non-squamous non-small cell lung cancer. Paraffin-embedded, formalin-fixed specimens were used for these analyses. Laser microdissection (Leica DM6000B, Leica, Solms, Germany) was performed on the biggest available tumor cell aggregates to increase DNA extraction quality and quantity at the boundary between healthy and pathological bone area. We obtained two DNA extraction tubes containing about 500 000  $\mu\text{m}^2$  of tumor cells each. DNA extraction was performed, and DNA concentration of 1–3  $\text{ng } \mu\text{l}^{-1}$  was obtained for each sample (QIAmp DNA microkit, Qiagen, Venlo, The Netherlands). DNA quality was assessed by nanodrop and gel electrophoresis. For *EGFR* (exons 18 to 21), *BRAF* (exons 11 and 15), *PIK3CA* (exons 10 and 21) and *HER2* (exon 20) genes, multiplex PCR reactions were performed using primers listed in Supplementary Table 1. Briefly, after agarose gels migration, PCR products were purified and used for PCR sequencing. Sanger sequencing was completed on ABI PRISM 3730xl sequencing apparatus (Applied Biosystems, Foster City, CA, USA). DNA samples were then used to look for *KRAS* mutation by SNaPshot procedure (Applied Biosystem). Finally, two 3- $\mu\text{m}$  paraffin-embedded blocks sections were used for ALK immunohistochemistry as described above, completed by fluorescent *in situ* hybridization (Vysis break-apart probe, Abbott Molecular, North Chicago, IL, USA) as described previously.<sup>20</sup>

Supplementary Information accompanies the paper on the BoneKEy website (<http://www.nature.com/bonekey>)

### Conflict of Interest

The authors declare no conflict of interest.

### Acknowledgements

This study is supported by a 2011 Young Investigator Grant from the Hospices Civils de Lyon, France, to CBC. We thank B Dubois, D Goehrig, S Geraci, Drs R Chapurlat, C Ferraro-Peyret, A Fontana, MO Joly, A Ltaief-Boudrigua, L Manera, A Martinon, B Etienne-Mastroianni, M Rabeyrin, AC Ravel, T Rolland, JY Scoazec, G Vaz, E Vignot and V Vo-Hoang for their help in patient management.

### References

1. Azzoli CG, Temin S, Aliff T, Baker Jr S, Brahmer J, Johnson DH *et al*. 2011 Focused Update of 2009 American Society of Clinical Oncology Clinical Practice Guideline Update on Chemotherapy for Stage IV Non-Small-Cell Lung Cancer. *J Clin Oncol* 2011;**29**:3825–3831.
2. Pao W, Girard N. New driver mutations in non-small-cell lung cancer. *Lancet Oncol* 2011;**12**:175–180.
3. Van Allen EM, Wagle N, Stojanov P, Perrin DL, Cibulskis K, Marlow S *et al*. Whole-exome sequencing and clinical interpretation of formalin-fixed, paraffin-embedded tumor samples to guide precision cancer medicine. *Nat Med* 2014;**20**:682–688.
4. Coleman RE. Clinical features of metastatic bone disease and risk of skeletal morbidity. *Clin Cancer Res* 2006;**12**:6243s–6249s.
5. Decroisette C, Monnet I, Berard H, Quere G, Le Caer H, Bota S *et al*. Epidemiology and treatment costs of bone metastases from lung cancer: a French prospective, observational, multicenter study (GFPC 0601). *J Thorac Oncol* 2011;**6**:576–582.
6. Nottebaert M, Exner GU, von Hochstetter AR, Schreiber A. Metastatic bone disease from occult carcinoma: a profile. *Int Orthop* 1989;**13**:119–123.
7. Alers JC, Krijtenburg PJ, Vissers KJ, van Dekken H. Effect of bone decalcification procedures on DNA *in situ* hybridization and comparative genomic hybridization. EDTA is highly preferable to a routinely used acid decalcifier. *J Histochem Cytochem* 1999;**47**:703–710.
8. Brown RS, Edwards J, Bartlett JW, Jones C, Dogan A. Routine acid decalcification of bone marrow samples can preserve DNA for FISH and CGH studies in metastatic prostate cancer. *J Histochem Cytochem* 2002;**50**:113–115.
9. Mukai K, Yoshimura S, Anzai M. Effects of decalcification on immunoperoxidase staining. *Am J Surg Pathol* 1986;**10**:413–419.
10. Neves Jdos S, Omar NF, Narvaes EA, Gomes JR, Novaes PD. Influence of different decalcifying agents on EGFR and EGFR immunostaining. *Acta Histochem* 2011;**113**:484–488.
11. Singh VM, Salunga RC, Huang VJ, Tran Y, Erlander M, Plumlee P *et al*. Analysis of the effect of various decalcification agents on the quantity and quality of nucleic acid (DNA and RNA) recovered from bone biopsies. *Ann Diagn Pathol* 2013;**17**:322–326.
12. Barlesi F, Blons H, Beau-Faller M, Rouquette I, Ouafik L, Mosser J *et al*. Biomarkers (BM) France: Results of routine EGFR, HER2, KRAS, BRAF, PI3KCA mutations detection and EML4-ALK gene fusion assessment on the first 10,000 non-small cell lung cancer (NSCLC) patients (pts). *J Clin Oncol* 2013;**31**(suppl):abstr 8000.
13. Bauml J, Mick R, Zhang Y, Watt CD, Vachani A, Aggarwal C *et al*. Determinants of survival in advanced non-small-cell lung cancer in the era of targeted therapies. *Clin Lung Cancer* 2013;**14**:581–591.
14. Cadranel J, Mauguen A, Faller M, Zalzman G, Buisine M-P, Westeel V *et al*. Impact of systematic EGFR and KRAS mutation evaluation on progression-free survival and overall survival in patients with advanced non-small-cell lung cancer treated by erlotinib in a French prospective cohort (ERMETIC project-part 2). *J Thorac Oncol* 2012;**7**:1490–1502.
15. Doebele RC, Lu X, Sumey C, Maxson DA, Weickhardt AJ, Oton AB *et al*. Oncogene status predicts patterns of metastatic spread in treatment-naive nonsmall cell lung cancer. *Cancer* 2012;**118**:4502–4511.
16. Garfield D. Increasing osteoblastic lesions as a manifestation of a major response to gefitinib. *J Thorac Oncol* 2006;**1**:859–860.
17. Sun JM, Ahn JS, Lee S, Kim JA, Lee J, Park YH *et al*. Predictors of skeletal-related events in non-small cell lung cancer patients with bone metastases. *Lung Cancer* 2011;**71**:89–93.
18. Lu X, Wang Q, Hu G, Van Poznak C, Fleisher M, Reiss M *et al*. ADAMTS1 and MMP1 proteolytically engage EGF-like ligands in an osteolytic signaling cascade for bone metastasis. *Genes Dev* 2009;**23**:1882–1894.
19. Canon J, Bryant R, Roudier M, Osgood T, Jones J, Miller R *et al*. Inhibition of RANKL increases the anti-tumor effect of the EGFR inhibitor panitumumab in a murine model of bone metastasis. *Bone* 2010;**46**:1613–1619.
20. McLeer-Florin A, Moro-Sibilot D, Melis A, Salameire D, Lefebvre C, Ceccaldi F *et al*. Dual IHC and FISH testing for ALK gene rearrangement in lung adenocarcinomas in a routine practice: a French study. *J Thorac Oncol* 2012;**7**:348–354.